Supplementary Information

Bona fide stochastic resonance under nonGaussian active fluctuations

Govind Paneru[ab], Tsvi Tlusty*[ab], and Hyuk Kyu Pak*[ab]

[1]Center for Soft and Living Matter, Institute for Basic Science (IBS), Ulsan 44919, Republic of Korea

[2]Department of Physics, Ulsan National Institute of Science and Technology, Ulsan 44919, Republic of Korea

Active noise generation procedure

The active noise in the main text is generated numerically as follows: Let Q_n be the sequence of identically distributed random numbers that follow a Gaussian distribution with variance σ^2,

$$P(Q) = \frac{1}{\sqrt{2\pi\sigma^2}} \exp(-\frac{Q^2}{2\sigma^2}). \tag{S1}$$

From these random numbers, we can generate a sequence of random numbers that follow a nonGaussian distribution (Fig. S1 (a)):

$$q_P(t) = \sum_{i=1} Q_i \delta(t - t_i). \tag{S2}$$

Here, each kick of duration $\Delta t \to 0$ arrives at a random interval t_i following a Poisson distribution. The kick arrival time (time interval between successive kicks) thus follows the Poisson distribution with mean arrival time $\tau_P = \overline{t_{i+1} - t_i}$. Eq. S2 shows all random numbers of the sequence Q_n from white Gaussian noise becomes zero except one arriving at the *i*th interval t_i; hence, the variance of the nonGaussian white noise q_P is given by $\sigma^2/(1+\tau_P/\Delta t)$. The exponentially correlated nonGaussian noise $y(t)$ of correlation time τ_c can be generated recursively using the following relation [1],

$$y(t+\Delta t) = \exp(-\Delta t/\tau_c)\ \ y(t) + \sqrt{1-\exp(-2\Delta t/\tau_c)}\ \ q_P(t+\Delta t). \tag{S3}$$

The time traces of the exponentially correlated nonGaussian active noise $y(t)$ are shown in Fig. S1(b). The active force $\xi_{act}(t)$ is obtained by multiplying $y(t)$ with the trap stiffness k as

$$\xi_{act}(t) = ky(t). \tag{S4}$$

The above noise generation approach is equivalent to the active Ornstein–Uhlenbeck process[2]:

$$\tau_c d\xi_{act}(t)/dt = -\xi_{act}(t) + \sqrt{2}\xi_{PN}(t), \tag{S5}$$

where $\xi_{PN}(t)$ is the nonGaussian white noise with a zero mean $\langle \xi_{PN}(t) \rangle = 0$ and correlation $\langle \xi_{PN}(t)\xi_{PN}(t') \rangle = [\mathrm{A}/(1+\tau_P/\Delta t)]\delta(t-t')$; and A is the energy scale of the active force. The Kurtosis $K(t) = <[\xi(t) - <\xi(t)>]^4> / <[\xi(t) - <\xi(t)>]^2>^2$, which measures the degree of nonGaussianity of the probability distributions, of nonGaussian white noise $\xi_{PN}(t)$ and the exponentially correlated active noise $\xi_{act}(t)$, are shown in Fig. S1(d) and Fig. S1(e), respectively. The active noise $\xi_{act}(t)$ becomes nonGaussian ($K > 3$) for $\tau_P/\tau_c \gtrsim 0.2$. Integrating Eq. (S5), we get the formal solution for the nonGaussian active noise:

$$\xi_{act}(t) = \xi_{act}(0)e^{-t/\tau_c} + \frac{\sqrt{2}}{\tau_c}\int_0^t e^{-(t-t')/\tau_c}\xi_{PN}(t')dt'. \quad \text{(S6)}$$

From Eq. (S6), we can derive the autocorrelation of the nonGaussian active noise as

$$\left\langle \xi_{act}(t)\xi_{act}(t')\right\rangle = \left\langle (\xi_{act}(0))^2\right\rangle e^{-(t+t')/\tau_c} + \frac{2}{\tau_c^2}\int_0^t ds e^{-(t-s)/\tau_c}\int_0^{t'} ds' e^{-(t'-s')/\tau_c}\left\langle \xi_{PN}(s)\xi_{PN}(s')\right\rangle. \quad \text{(S7)}$$

By using $\left\langle \xi_{PN}(s)\xi_{PN}(s')\right\rangle = [\mathrm{A}/(1+\tau_P/\Delta t)]\delta(s-s')$, Eq. S7 becomes

$$\left\langle \xi_{act}(t)\xi_{act}(t')\right\rangle = \left\langle (\xi_{act}(0))^2\right\rangle e^{-(t+t')/\tau_c} + \frac{\mathrm{A}/(1+\tau_P/\Delta t)}{\tau_c}[e^{(t-t')/\tau_c} - e^{-(t+t')/\tau_c}]. \quad \text{(S8)}$$

In steady state, $\left\langle (\xi_{act}(0))^2\right\rangle$ is equal to the variance of the active noise, $\left\langle (\xi_{act}(t))^2\right\rangle = \mathrm{A}/[\tau_c(1+\tau_P/\Delta t)]$. Hence, the autocorrelation of the nonGaussian active noise in steady state is given by

$$\left\langle \xi_{act}(t)\xi_{act}(t')\right\rangle = \frac{\mathrm{A}/(1+\tau_P/\Delta t)}{\tau_c}e^{-|t-t'|/\tau_c}. \quad \text{(S9)}$$

The active force strength $f_{act} \equiv \sqrt{C/(1+\tau_P/\Delta t)}$ of the nonGaussian active noise is related to A and τ_c as $f_{act} = \sqrt{\mathrm{A}/[\tau_c(1+\tau_P/\Delta t)]}$. For $\tau_P \to 0$ and $\Delta t \to 0$, $\mathrm{A}/(1+\tau_P/\Delta t) \to \mathrm{A}$, hence $\xi_{PN}(t)$ reduces to the Gaussian white noise ξ_{GN} of zero mean and correlation $\left\langle \xi_{GN}(t)\xi_{GN}(t')\right\rangle = \mathrm{A}\delta(t-t')$ and the active noise $\xi_{act}(t)$ in Eq. (S5) reduces to the active Ornstein–Uhlenbeck noise with correlation $\left\langle \xi(t)\xi(t')\right\rangle_{OU} = (\mathrm{A}/\tau_c)e^{-|t-t'|/\tau_c}$.

Solving Eq. (S5) by the Fourier transform method, we can derive an expression for the power spectral density (PSD) of the nonGaussian active noise:

$$S(\omega) = \frac{2f_{act}^2\tau_c}{1+\tau_c^2\omega^2}. \quad \text{(S10)}$$

Figure S1(f) shows the PSD of the nonGaussian active noise agrees well with Eq. (S10).

Particle dynamics in a harmonic potential

We consider the one-dimensional motion of the particle in a harmonic potential $V(x) = (1/2)kx^2$ in an active bath. The motion of the particle is given by the overdamped Langevin equation:

$$\gamma\frac{dx}{dt} = -kx + \xi_{th} + \xi_{act}. \quad \text{(S11)}$$

The mean squared displacement (MSD) of the particle in the harmonic potential during the time interval t in steady-state can be calculated by solving Eq. (S11) by Laplace transform method [3]:

$$\left\langle \Delta x^2(t)\right\rangle = 2D\tau_r\left(1-\mathrm{e}^{-t/\tau_r}\right) + \frac{2\mathrm{A}\tau_r}{\gamma^2(1+\tau_P/\Delta t)}\frac{\left[1-\mathrm{e}^{-t/\tau_r} - (\tau_c/\tau_r)\left(1-\mathrm{e}^{-t/\tau_c}\right)\right]}{[1-(\tau_c/\tau_r)^2]}. \quad \text{(S12)}$$

Figure S5(c) shows that the MSD of the particle in the presence of nonGaussian active noise fits well with Eq. (S12). Also, we show that the MSD with nonGaussian active noise coincides with the MSD of the AOU noise of the same

f_{act} and τ_c. Thus, the steady state dynamics in the presence of nonGaussian active noise is similar to that of the AOU noise.

Figures

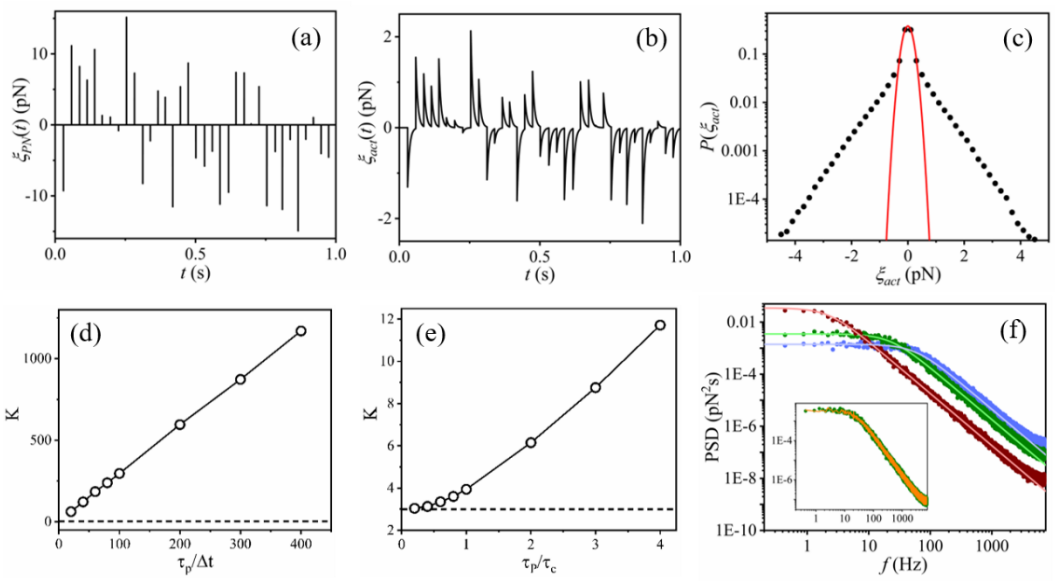

Fig. S1. (a) Trace of the nonGaussian white noise $\xi_{PN}(t)$ with $\tau_P = 28$ ms generated from Gaussian white noise of variance $C = k^2\sigma^2 = (10\text{ pN})^2$, following Eq. (S2). The variance of the nonGaussian white noise is given by $C/(1+\tau_P/\Delta t) \approx (0.5\text{ pN})^2$. The average waiting time between the kicks is τ_P. Note that although each kick arrives at an average interval τ_P, the strength and direction of the kicks are purely random, which follow white Gaussian noise. (b) The exponentially correlated nonGaussian active noise $\xi_{act}(t)$ of strength $f_{act} \equiv \sqrt{C/(1+\tau_P/\Delta t)} \approx 0.5$ pN with $\tau_P = 28$ ms and $\tau_c = 7$ ms generated from the nonGaussian white noise in panel (a) using Eq. (S4). (c) Probability distribution function (PDF) of the nonGaussian active noise in panel (b). The solid red curve is the Gaussian fitting. (d) Kurtosis of the nonGaussian white noise as a function of $\tau_P/\Delta t$. (e) Kurtosis of nonGaussian active noise as a function of τ_P/τ_c. The horizontal dashed line in (d) and (e) correspond to Gaussian distribution $K = 3$. (f) Power spectral density (PSD) of the nonGaussian active noise of fixed $f_{act} = 0.5$ pN and $\tau_P = 28$ ms with $\tau_c = 2.8$ ms (blue), 7 ms (olive), and 70 ms (wine). The solid curves are the theoretical plots using Eq. (S10). Inset: PSD of the nonGaussian active noise of $f_{act} = 0.5$ pN, $\tau_P = 28$ ms, and $\tau_c = 7$ ms (olive) coincides with the active Ornstein–Uhlenbeck noise of same strength $f_{act} = 0.5$ pN and correlation time $\tau_c = 7$ ms (orange).

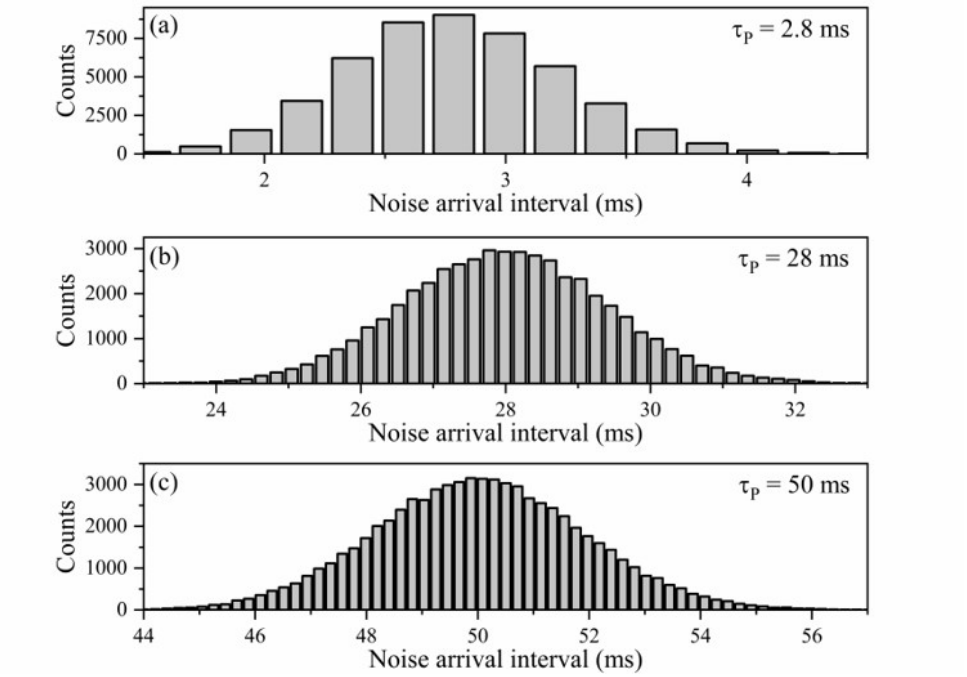

Fig. S2. Noise arrival time distribution for nonGaussian active noise follows a Poisson distribution with average noise arrival time (a) $\tau_P = (2.8 \pm 0.44)$ ms , (b) $\tau_P = (28 \pm 1.41)$ ms , and (c) $\tau_P = (50 \pm 1.88)$ ms .

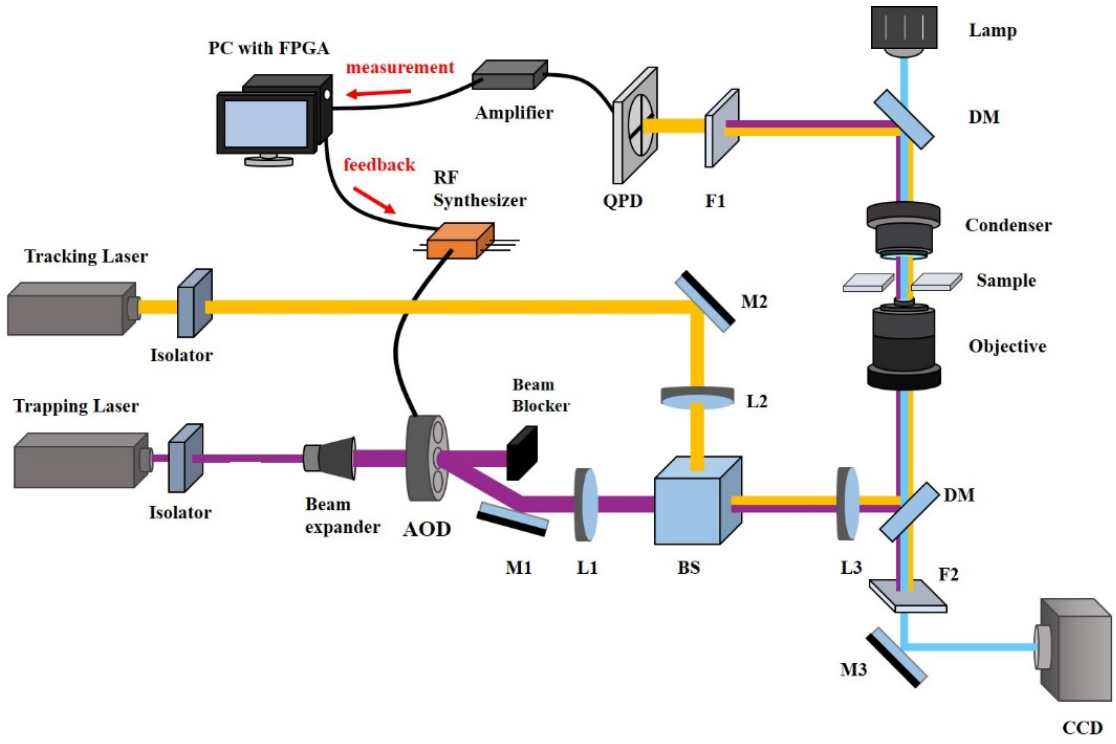

Fig. S3. Schematics of the active optical feedback trap (AOFT) setup. M1, M2, M3: mirror. L1, L2, L3: Lens. BS: beam splitter, DM: dichroic mirror, F1, F2: filter. CCD: camera.

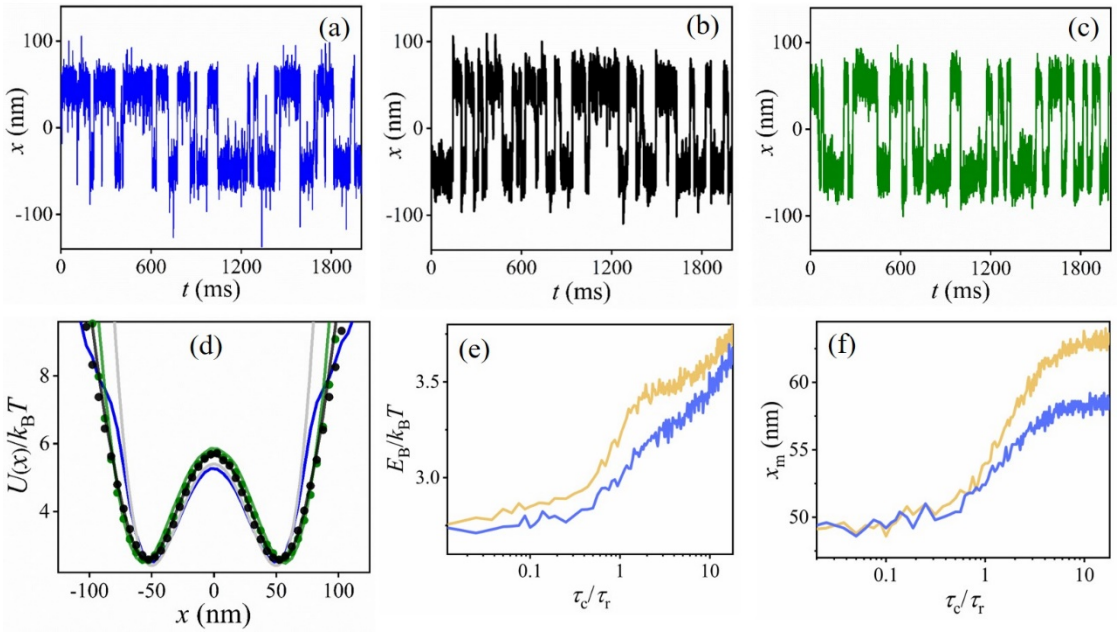

Fig. S4. Trajectories of the particle in a double-well potential, $E_b/k_BT = 3$ and $x_m = 50$ nm (top panels), in the presence of nonGaussian active noise of fixed strength $f_{act} \approx 0.5$ pN and average noise arrival time $\tau_P \approx 28$ ms with correlation time (bottom panels). (a) $\tau_c \approx 0.28$ ms (blue, numerical result), (b) 7 ms (black), and (c) 21 ms (green). The PDFs of the particle position in Fig. 1b of the main text are from these trajectories. (d) Effective double-well potentials $U(x)/k_BT \sim -\ln P(x)$ for the like-colored data in panels (a) to (c) (also PDFs in Fig. 1b in the main text). The dotted curves represent the experimental results. The solid curves are obtained from the numerical simulation of Eq. (1) in the main text. The gray curve is the theoretical plot of the symmetric double-well potential with $E_b/k_BT = 3$ and $x_m = 50$ nm. (Numerical result) (e)-(f) Plot showing the variation of the barrier height E_b/k_BT and well separation x_m as a function of τ_c/τ_r for the particle in symmetric double-well with $E_b/k_BT = 3$ and $x_m = 50$ nm in the presence of the nonGaussian active noise with $\tau_P = 20$ ms and $f_{act} = 0.5$ pN (blue) and $f_{act} = 1$ pN (orange).

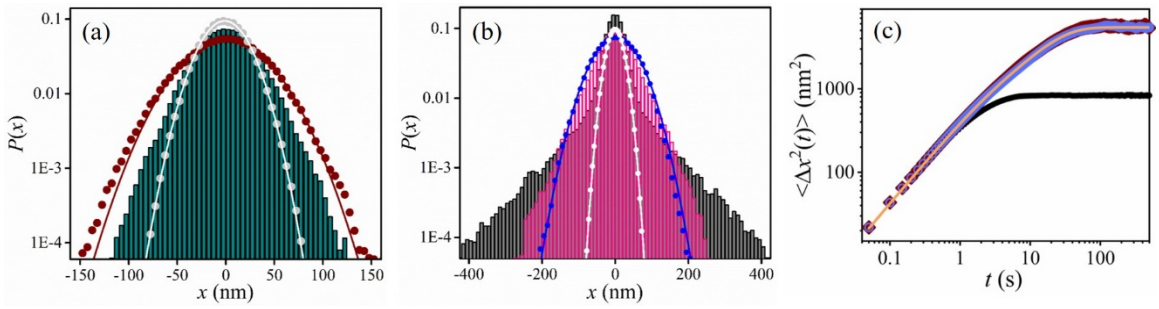

Fig. S5. PDF of the particle position in harmonic potential $V_{op}(x) = (k/2)(x - x_c)^2$ in the presence of nonGaussian active noise. Here, the active noise is injected into the particle in the form of feedback force $f_{act}(t) = -ky(t)$ that corresponds to the shift of the potential center by $x_c(t) = x(t) - y(t)$. (a) (experimental result) PDF of the particle position in the harmonic potential of stiffness $k \approx 9.1$ pNμm^{-1} in the thermal bath (gray circles), in the presence of

non-Gaussian noise of strength $\sqrt{C} = 4.6$ pN and correlation time $\tau_c = 17.5$ ms with noise arrival interval $\tau_P = 14$ ms (wine circles), and 35 ms (dark cyan bars). The solid curves are the Gaussian fittings. (b) (numerical result obtained by solving Eq. S11) PDF of the particle position in the harmonic potential in the thermal bath (white circles), in the presence of non-Gaussian noise of fixed strength $f_{act} = 0.5$ pN and correlation time $\tau_c = 25$ ms with $\tau_P = 5$ ms (blue circles), 50 ms (pink bars), and 250 ms (black bars). The solid curves are the Gaussian fittings. We found that the PDFs are non-Gaussian only when $\tau_c \lesssim \tau_P$ and $f_{act} \gtrsim f_{th}$, where $f_{th} = \sqrt{k_B T k} \approx 0.2$ pN is the thermal strength. (c) Mean squared displacement of a particle in the harmonic potential in steady-state in the presence of the nonGaussian active noise of $f_{act} = 0.5$ pN, $\tau_c = 20$ ms, and $\tau_P = 40$ ms (light blue) coincides with the MSD in the presence of AOU noise of same $f_{act} = 0.5$ pN and $\tau_c = 20$ ms (wine). The orange solid curve is the plot of Eq. (S12). The black data is the MSD in the thermal bath.

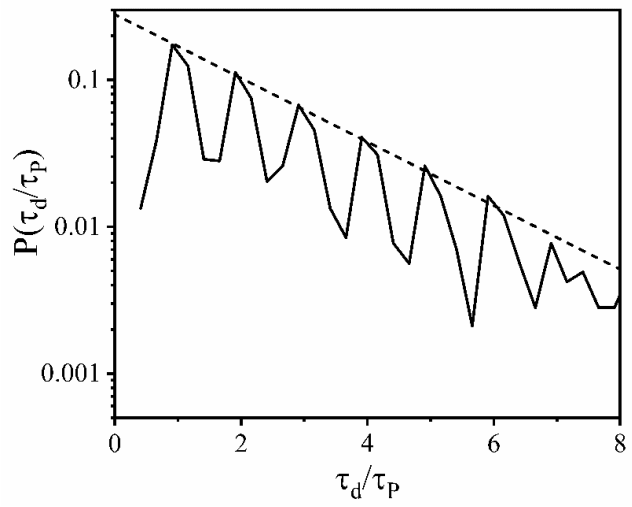

Fig. S6. Semi-log plot of the residence time distribution of the particle in the symmetric double-well potential in the presence of nonGaussian active noise of $f_{act} \approx 1$ pN and $\tau_c / \tau_P \approx 0.25$. The dotted line corresponds to $y = 0.28\exp(-0.5x)$. The fitting of the dotted line with the peak heights demonstrates that the height of each peak decreases exponentially with their order n.

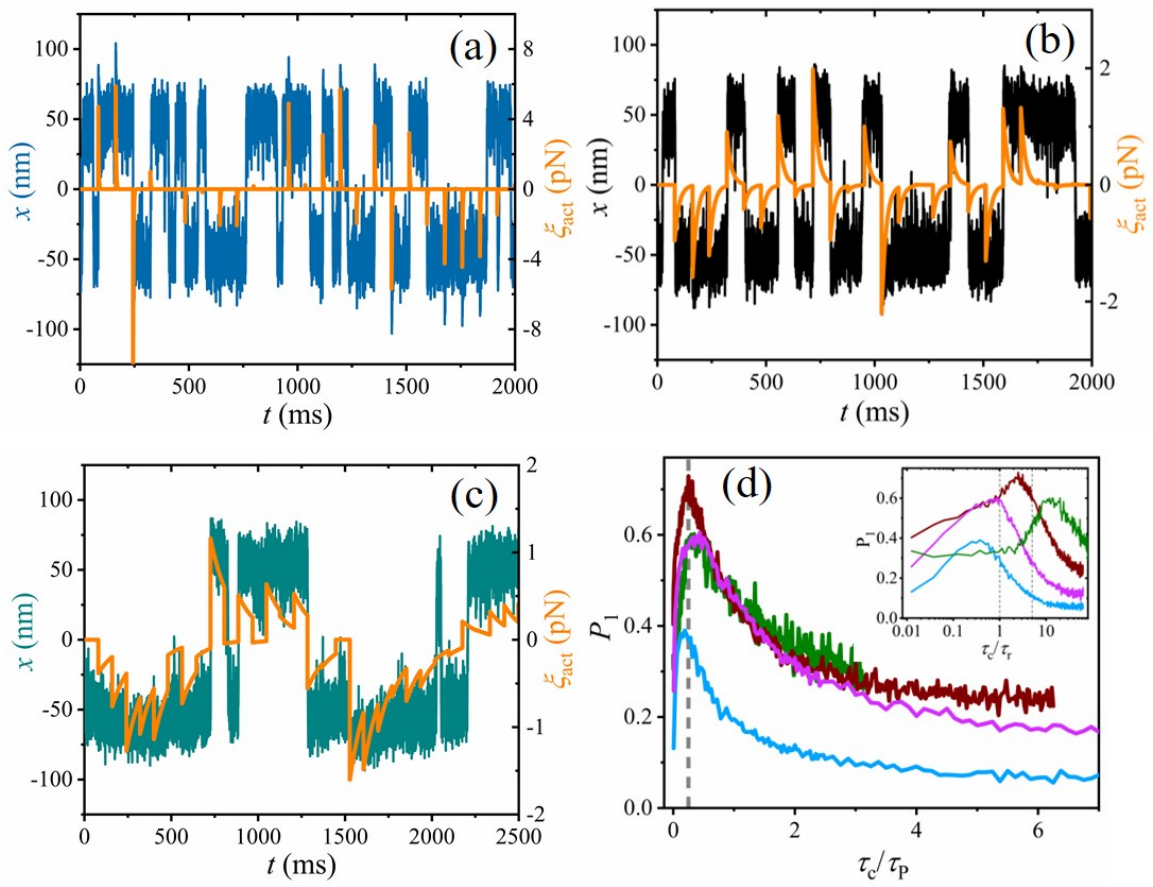

Fig. S7. (Numerical result obtained by solving Eq. (1) in the main text) (a) to (c) Particle trajectories and nonGaussian active noise trajectories (orange curves) for the motion of the particle in the double well potential in the presence of nonGaussian active noise of fixed $f_{act} \approx 0.5$ pN and $\tau_P / \tau_r \approx 20$ with (a) $\tau_c / \tau_r \approx 0.5$, (b) $\tau_c / \tau_r \approx 5$, and (c) $\tau_c / \tau_r \approx 30$. (d) Plot of the first peak strength P_1 as a function of τ_c / τ_P for fixed $f_{act} \approx 0.5$ pN and $\tau_P \approx 8$ ms (light blue) $\tau_P \approx 16$ ms (light purple), $\tau_P \approx 40$ ms (wine), and $\tau_P \approx 160$ ms (olive). For all cases, P_1 is maximum near $\tau_c / \tau_P \approx 0.25$ (dashed vertical line). Inset: Same data in the main panel plotted as a function of τ_c / τ_r shows the global maximum of P_1 is when $\tau_r < \tau_c \lesssim 5\tau_r$.

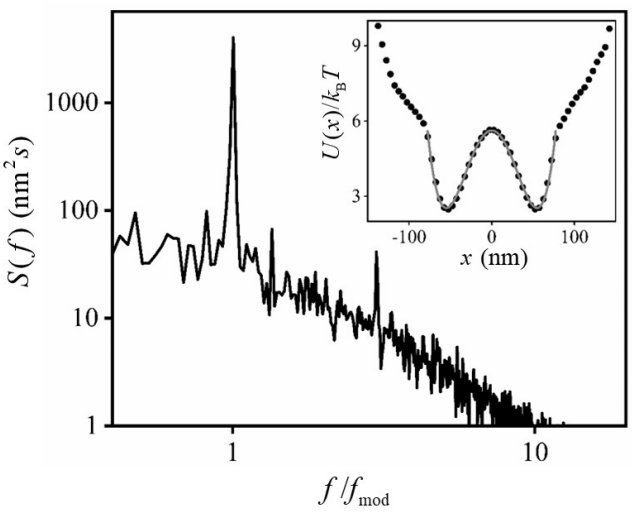

Fig. S8. (Numerical result obtained by solving Eq. (1) in the main text) Power spectral density in the presence of the nonGaussian active noise of strength $f_{act} \approx 1$ pN (greater than thermal strength $f_{th} \approx 0.4$ pN) with $\tau_c \approx 25$ ms and $\tau_P \approx 1000$ ms (non-Gaussian regime), under the same resonant condition of Fig. 3(c) in the main text. Inset: the effective double-well potential (black circles) for the same data in the main panel. The gray solid curve fits well with the symmetric double-well potential $V_{DW}(x)$ of $E_b/k_BT = 3$ and $x_m = 50$ nm with the fitting parameter $E_b/k_BT = 3.09 \pm 0.06$ and $x_m = 54.9 \pm 0.2$ nm, showing that the effective double-well potential follows Gaussian distribution near the center with non-Gaussian outer tails.

1. M. Deserno, *[https://www.cmu.edu/biolphys/deserno/pdf/corr_gaussian_random.pdf]*.
2. A. K. Tripathi, T. Das, G. Paneru, H. K. Pak and T. Tlusty, *Communications Physics*, 2022, **5**, 101.
3. C. Maggi, M. Paoluzzi, N. Pellicciotta, A. Lepore, L. Angelani and R. Di Leonardo, *Physical Review Letters*, 2014, **113**, 238303.